Novel proton conductors in the layered oxide material LixlAl0. 5Co0. 5O2

Lan, R & Tao, S

Original citation & hyperlink:
Lan, R & Tao, S 2014, 'Novel proton conductors in the layered oxide material LixlAl0. 5Co0. 5O2' *Advanced Energy Materials*, vol 4, no. 7, 1301683
https://dx.doi.org/10.1002/aenm.201301683

DOI 10.1002/aenm.201301683
ISSN 1614-6832
ESSN 1614-6840

Publisher: Wiley

Novel proton conductors in layered oxide material $Li_xAl_{0.5}Co_{0.5}O_2$

Rong Lan and Shanwen Tao*

Department of Chemical & Process Engineering, University of Strathclyde, Glasgow G1 1XJ, UK

To identify a good ionic conducting material for use as electrolyte for intermediate temperature solid oxide fuel cells (IT-SOFCs) remains a big challenge. In this report, we demonstrate that good proton conductor can be obtained in transition element rich intercalation materials such as $Li_xAl_{0.5}Co_{0.5}O_2$. OCV of 1.0 ~ 1.1V was observed for a H_2/air fuel cell at temperature 475 – 575 °C indicating it is nearly a pure ionic conductor under fuel cell operating conditions. A power density of 173 mW cm^{-2} has been achieved at 525 °C with a thick electrolyte (0.79 mm thick) when silver was used as both cathode and anode. The ionic conductivity of $LiAl_{0.5}Co_{0.5}O_2$ was 0.1 S/cm at 500 °C, deduced from the series resistance of the H_2/air fuel cell. This is the highest among known poly-crystalline proton-conducting materials. This study will provide a new approach to discover new proton conducting materials for use in IT-SOFCs.

Proton conducting oxides are key materials for fuel cells; however, there is a gap in the temperature range of 200 - 600 °C.[1] There are some reports on intermediate temperature proton conducting materials such as CsH_2PO_4,[2] ammonium polyphosphate [3-6] and In-doped SnP_2O_7 are reported to be good proton conductors.[7-11] It is believed that, to some extent, the proton conduction of these materials are related to the presence of HPO_3 or H_3PO_4.[3, 10-12] Basically it is a kind of phosphoric acid fuel cell and the leaching or slow evaporation of these acids under fuel cell operating temperature could be a problem. High temperature proton conducting materials in solid oxides based on $BaCeO_3$ and $BaZrO_3$ have been widely investigated since the pioneer work reported by Iwahara et al. in 1981.[13-20] It has been reported that doped $LaPO_4$ and $LaNbO_4$ also exhibit reasonable proton conductivity;[21, 22] however, the proton conductivities of these oxides are not high enough to be used at intermediate temperature fuel cells. Therefore to discover new proton-conducting electrolytes for intermediate temperature solid oxide fuel cells (IT-SOFCs) remains a big challenge.

The conduction mechanism of these proton conducting oxides are related to defects, typically oxygen vacancies. The protons are introduced to these materials through the interaction between steam and these defects, or so-called extrinsic protons. On the other hand, there are some solid acids based on titanates or noibates such as $H_2Ti_3O_7$ [23] and $HPb_2Nb_3O_{10}{\cdot}nH_2O$ [24] which contains intrinsic protons. The measured conductivity of $H_2Ti_3O_7$ was 2.66 x 10^{-6} S cm^{-1} at 200 °C [23] whist for $HPb_2Nb_3O_{10}{\cdot}nH_2O$ the reported highest conductivity was 4.9 x 10^{-5} S cm^{-1} at 42 °C.[24] The low proton conductivity of these intrinsic proton containing oxides has discouraged researchers to keep searching for proton conducting materials in these solid acids. One possible reason of the low proton conductivity in solid acid such as in $H_2Ti_3O_7$ is due to the lack of suitable mobile channels.

Intercalation materials such as $LiCoO_2$, $LiFeO_2$, $LiNiO_2$ contain channels where cations such as Li^+ ions can move smoothly.[25-28] These materials are widely used as cathode in lithium ion batteries due to their excellent mixed Li^+/e' conduction. However, not only Li^+ ions, protons can also be intercalated into these layered oxides.[29] In this report, starting from layer $LiCoO_2$ (also called HT-$LiCoO_2$), we use following strategies to obtain a good proton conductor in intercalation oxides:

(1) To replace some cobalt by more stable element such as aluminium. Hopefully this will reduce the electronic conduction and provide a stable sub-lattice matrix in order to retain the layered structure with the channels for smooth migration of protons. This strategy has been successfully used to identify redox stable anode $(La_{0.75}Sr_{0.25})Cr_{0.5}Mn_{0.5}O_{3-\delta}$ for SOFCs.[30] α-$LiAlO_2$ is also a layer oxide with iso-structure to HT-$LiCoO_2$ therefore aluminium is an ideal dopant. At high temperatures, it is expected that H_2 at anode will loss electrons to form H^+ ions, the formed H^+ will *in situ* insert into the Li_xCoO_2 lattice to form $Li_xH_yCoO_2$. The charge balance for this process will be maintained either by reducing the charge of cobalt or by obtaining oxygen from the environment;

(2) To change the oxidation states of transition elements so as to supress the electronic conduction. It has been reported that bulk CoO exhibits antiferromagnetic properties and electronic insulator indicates the electrons are in pairs (low spin state).[31] The excessive positively charge introduced by protons will be balanced by the reduction of Co^{4+} ions to Co^{3+} or even to Co^{2+}. Another way to achieve charge balance is to fill in possible oxygen vacancies by absorbing oxygen from the environment but this is unlikely to happen at the fuel cell anode

due to the low oxygen partial pressure. At high temperatures, in the presence of fuels such as hydrogen at anode, if element cobalt in oxides is reduced to Co^{2+} ions, it is likely to get rid of electronic conduction thus the oxides become ionic conducing materials, suitable to be used as electrolytes for fuel cells.

It has been reported that β-H_xCoO_2 can be formed through treatment of layered $Na_{0.6}CoO_2$ in nitric acid.[29] Similarly, protons can be inserted into the layers of lithium deficient oxide $Li_xAl_{0.5}Co_{0.5}O_2$ to form $Li_xH_yAl_{0.5}Co_{0.5}O_2$ in the presence of hydrogen at high temperature. At the same time, some cobalt ions are reduced to lower valence state which allows the intercalation of protons in the lattice for charge compensation.

$$Li_xAl_{0.5}Co_{0.5}O_2 + y/2H_2 \rightarrow Li_xH_yAl_{0.5}Co_{0.5}O_2 \quad (1)$$

It is expected that the *in situ* formed $Li_xH_yAl_{0.5}Co_{0.5}O_2$ will have high proton conductivity due to the special structure and high temperature. The strategy for proton insertion in layered $Li_xAl_{0.5}Co_{0.5}O_2$ is shown in Figure 1.

Based on these strategies, we have successfully synthesised single phase oxide with nominal composition $LiAl_{0.5}Co_{0.5}O_2$. The room temperature XRD pattern of sample $LiAl_{0.5}Co_{0.5}O_2$ is shown in Figure S1. It is a trigonal system with the space group of $R\bar{3}m(166)$, with a = 2.8016(7) Å, c = 14.1631(34) Å, V = 96.28(4) $Å^3$ (Table S1) the same structure as reported for $LiAl_{0.5}Co_{0.5}O_2$ with comparable lattice parameters.[32] In this structure, cobalt and aluminium ions share the (0,0,1/2) sites which means random distribution of these ions at the B-sites.

The oxide with nominal composition $LiAl_{0.5}Co_{0.5}O_2$ is lithium deficient due to loss of lithium during the high temperature firing. The accurate formula is actually $Li_xAl_{0.5}Co_{0.5}O_2$ with x < 1.0. In terms of proton insertion, lithium deficient oxide will be a better choice. Therefore oxide with nominal composition $Li_{0.9}Al_{0.5}Co_{0.5}O_2$ and $Li_{0.8}Al_{0.5}Co_{0.5}O_2$ were also synthesised by the same method as described above. It was found that one extra peak at ~ 37° appears in sample $Li_{0.9}Al_{0.5}Co_{0.5}O_2$ and another peak appear at 31.6° in sample $Li_{0.8}Al_{0.5}Co_{0.5}O_2$ (Figure S2). The extra peaks were indexed as Co_3O_4 (JCPDS No 01-080-1541). As both $Li_{0.9}Al_{0.5}Co_{0.5}O_2$ and $Li_{0.8}Al_{0.5}Co_{0.5}O_2$ contain second phase Co_3O_4, our investigation focused on $LiAl_{0.5}Co_{0.5}O_2$. The main phase of sample $Li_{0.9}Al_{0.5}Co_{0.5}O_2$ also exhibits the same structure (Figure S3) as $LiCo_{0.5}Al_{0.5}O_2$ with similar lattice parameters (Table S2).

The conductivity of $LiCo_{0.5}Al_{0.5}O_2$ in air was measured from 700 to 200 °C on cooling. When the sample was held at 700 °C, the conductivity decreased first then started to increase and stabilised at 3.5×10^{-3} S/cm after 12 hour ageing (Figure 2A). According to thermal analysis, no obvious phase transition was observed up to 1000 °C (Figure S4A). However, slight weight loss between 600 and 1000 °C was observed which could be related to the loss of lattice oxygen or lithium-containing compounds. This could also be the reason for the conductivity change at 700 °C. The conductivity measured on cooling is shown in Figure 2B. The conductivity decreased at lower temperatures. At 500 °C, the total conductivity of nominal $LiCo_{0.5}Al_{0.5}O_2$ was 1.0×10^{-3} S/cm. The apparent conduction energy was 0.50(1) eV between 700-400 °C and 0.69(1) eV between 400-200 °C (Figure 2B); however, on the thermal analysis curves, there was no obvious weight change or thermal effect (Figure S4A). It is not clear what causes the change in conduction activation energy. The typical a.c. impedance spectrum is shown in Figure S5. The electrode response at low frequency was quite small indicating it could be a semi-conductor in air. It has been independently reported by Giorgi[33] and Tao[34] that the electric conductivity of HT - $LiCoO_2$ was 0.36 S/cm at 500 °C in air but it was dominated by electronic conduction. The reported conductivity for γ-$LiAlO_2$ was 1.3×10^{-6} S/cm at 500 °C.[35] To the best of our knowledge, there is no report on conductivity of α-$LiAlO_2$. The conductivity of nominal $LiCo_{0.5}Al_{0.5}O_2$ in air lies between $LiCoO_2$ and $LiAlO_2$.

In order to figure out the conduction mechanism of $LiAl_{0.5}Co_{0.5}O_2$ under fuel cell operating conditions, oxygen and hydrogen concentration cells were fabricated using silver as both cathode and anode. The ionic transfer number was calculated through the measured voltage and the calculated theoretical voltage according to Nernst equation. At 400 °C, the oxygen transfer number was about 1%, then gradually decreased to less than 0.2% at 725 °C. This experiment indicated that the oxygen conduction in $LiAl_{0.5}Co_{0.5}O_2$ is negligible. To confirm the proton insertion in the presence of hydrogen, the same cell was used for hydrogen concentration cell measurement. Between 400-500 °C, the proton transfer number was around 30% (Figure 3B). The proton transfer number gradually increased from 30 to 71% between 500 and 625 °C. After 625 °C, the transfer number decreased sharply, possibly due to the decomposition of the material which destroyed the structure. As silver is not an ideal reversible electrode for hydrogen, the measured transfer number could be relatively lower than real value. The proton conduction in layered oxide is anticipated to closely related to the difference in

hydrogen partial pressure at the two electrodes. The driving force between pure and 5%H_2 might not be high enough for efficient insertion of protons in the $Li_xAl_{0.5}Co_{0.5}O_2$ lattice therefore co-existence of Li^+ ion conduction is possible under the circumstance $Li_xAl_{0.5}Co_{0.5}O_2$ might not be a pure protonic conductor under hydrogen concentration cell conditions. However, under a H_2/air fuel cell condition, the driving force for insertion of protons at the anode side and extraction of protons at cathode side is so strong that protonic conduction becomes dominant under hydrogen fuel cell conditions. Thermal analyses of $LiAl_{0.5}Co_{0.5}O_2$ in 5%H_2/Ar indicated weight loss started at ~ 500 °C and became significant above 625 °C (Figure S4B). The weight loss could be related to the reduction of $LiAl_{0.5}Co_{0.5}O_2$.This is most likely due to the loss of oxygen through reduction of multi-valent element cobalt together with the *in situ* insertion of protons. From these experiments, it has been demonstrated that $LiAl_{0.5}Co_{0.5}O_2$ is a proton conductor in the presence of hydrogen at high temperature. Therefore the material is suitable to be used as electrolyte for fuel cells.

$LiAl_{0.5}Co_{0.5}O_2$ was used as electrolyte for a H_2/air fuel cell using silver as both anode and cathode as well as current collector. A Type A sandwich cell with dense layer of 100 μm and overall thickness 670μm was fabricated (Figure S7A). The fuel cell performance of this cell is shown in Figure S6. An OCV above 1.0V was observed during 475 – 575 °C. At 525 °C the maximum current and power density were 227 mA/cm^2 and 53 mW/cm^2 respectively. After fuel cell measurement, as can be observed from SEM, some loss of silver electrode at the anode surface was observed indicating the possible reaction between silver and $LiAl_{0.5}Co_{0.5}O_2$ (Figure S7B). On the other hand, the cathode surface looked fine indicating the possible reaction between silver and $LiAl_{0.5}Co_{0.5}O_2$ happened only in a reducing atmosphere (Figure S7C). At the cathode, oxidation of silver is not a problem as this process happens at a temperature below 250 °C which is lower than the operating temperature of IT-SOFCs.[36] In the sandwich cell, although the dense layer is quite thin, the porous layer may also facilitate gas diffusion, but real electrochemical reactions only happens on the surfaces in contact with silver. The real thickness of the electrolyte was 0.67mm while the voids in the porous layers may increase the overall resistance. From this point of view, with only a dense layer would be a better choice. Therefore we also fabricated Type B pellet cell directly using thick $LiAl_{0.5}Co_{0.5}O_2$ pellet as the electrolyte. The H_2/air fuel cell performance for this cell is shown in Figure 4A. The cell exhibited good performance between 475 and 575 °C. At 525 °C, the maximum current density and power density were 698mA/cm^2 and 173 mW/cm^2 respectively whist the thickness of the

electrolyte was 0.79 mm. The a.c. impedance spectra of the cell measured at OCV and different temperatures are shown in Figure 4B. The series resistance of the cell was around 0.5 Ω cm^2 between 475 and 550 °C. At 575 °C, the series resistance decreased, possible due to the interaction between electrolyte and silver at the anode (Figure S7B), leading to poor contact resistance. From the series resistance of the Type B cell, assuming the contact resistance between electrode and electrolyte is negligible, the ionic conductivity can be evaluated. As shown in Figure 2B, the ionic conductivity deduced from fuel cell impedance spectra is much higher than those measured in air. At 500 °C, under the fuel cell operating condition, the ionic conductivity of $LiAl_{0.5}Co_{0.5}O_2$ was 0.10 S/cm which was two orders of magnitude of that in air (1.04×10^{-3} S/cm). The difference is likely due to the high mobility of inserted protons in layered oxides. This value is comparable to that of 0.11S/cm for the grain boundary free $BaZr_{0:8}Y_{0:2}O_{3-\delta}$ film grown on MgO substrate by pulsed laser deposition method.[37] However, the $LiAl_{0.5}Co_{0.5}O_2$ in this study was in poly-crystalline, would be more feasible for fabrication of electrochemical devices on poly-crystalline or porous substrates. The ionic conductivity of the known best electrolyte for SOFCs, $(ZrO_2)_{0.9}(Y_2O_3)_{0.1}$ [38] and typical poly-crystalline proton conducting materials such as $La_{0.99}Ca_{0.01}NbO_4$,[21] $BaCe_{0.7}Zr_{0.1}Y_{0.2}O_{3-\delta}$,[20] $BaCe_{0.5}Zr_{0.3}Y_{0.16}Zn_{0.04}O_{3-\delta}$[17] and $BaZr_{0.8}Y_{0.2}O_{3-\delta}$[19] are also plotted for comparison (Figure 2B). In the temperature range of 475 – 550 °C, the ionic conductivity of $LiAl_{0.5}Co_{0.5}O_2$ is roughly one order of magnitude higher than those of the known best proton conducting poly-crystalline oxides. With further investigation and optimisation, it is probable to identify better protonic conductors in the layered oxides. The theoretical OCV of H_2/air fuel cell is 1.045V at 525 °C while observed OCV was 1.022 V. This indicated that $LiAl_{0.5}Co_{0.5}O_2$ is almost a pure H^+ or O^{2-} or mixed H^+/O^{2-} ionic conductor under H_2/air fuel cell operating conditions. In another word, Li^+ ion and electronic conduction in $LiAl_{0.5}Co_{0.5}O_2$ are negligible. Some extent of oxygen ion conduction seems possible due to possible formation of oxygen vacancies at the anode side when exposed to H_2, but the cathode side is open to air therefore the pathway for oxygen ions is blocked since $LiAl_{0.5}Co_{0.5}O_2$ does not conduct O^{2-} ions, evidenced from oxygen concentration cell measurement (Figure 3A). It is reasonable to say that $LiAl_{0.5}Co_{0.5}O_2$ is a proton conductor under hydrogen fuel cell operating conditions.

After the fuel cell measurement, the cell was cooled down to room temperature under protection of hydrogen. Room temperature XRD pattern indicates that the electrolyte partially decomposed to γ-$LiAlO_2$ (JCPDS 01-073-1338) and Co_3O_4 (JCPDS 01-076-1802) (Figure S8).

This implies that the loss of lithium at high temperature caused partial decomposition. To replace lithium by more stable elements such as sodium, potassium, may lead to a more stable proton conductor for use as electrolyte for IT-SOFCs.

In brief, a new family of proton conducting oxides based on intercalation oxide $LiCoO_2$ and the iso-structural oxide α-$LiAlO_2$ has been identified. Based on these materials, both sandwich and pellet type symmetrical solid oxide fuel cells using silver as both electrodes as well as current collector have been fabricated and reasonable power density (173 mW/cm^2 at 525 °C) has been obtained with a 0.79 mm thick electrolyte. A proton conductivity of 0.1 S/cm was observed at 500 °C for $LiAl_{0.5}Co_{0.5}O_2$ which is the highest among the reported proton-conducting poly-crystalline oxides at this temperature range. Similar phenomena have also been observed in other layered intercalation materials in our ongoing research. The proton conduction mechanism is believed related to the special layered structure, very different from the conventional perovskite or doped $LaNbO_4$ which are related to oxygen vacancies. This study provides a new approach to discover new proton conducting materials for intermediate temperature solid oxide fuel cells and other electrochemical devices. It also demonstrates the possibility in discovering new ionic conducting materials in oxides with a large amount of first row multi-valent transition elements such as cobalt in the crystal lattice.

Experimental section

The oxide was prepared by a combustion method as described in a previous report.[32] Calculated amounts of $LiNO_3$, $Al(NO_3)_3{\cdot}9H_2O$and $Co(NO_3)_3{\cdot}6H_2O$ was dissolved in de-ionic water. Then an appropriate amount of citric acid was added to form a mixed solution. The solution was heated at 80 °C until a gel is formed. The gel was pre-fired at 400 °C then further fired at 800 °C for 3 hours to obtained single phase materials. The as fired powders were pressed into pellets using dies with 13mm and 20mm in diameter then fire at 1050 °C for 1 hour for conductivity and concentration cell measurement respectively.

X-ray data were collected on a PANanalyticalX'Pert Pro in the Bragg-Brentano reflection geometry with a Ni-filtered Cu Kα source (1.5405 Å), fitted with a X'Celerator detector and an Empyrean CuLFF xrd tube. Absolute scans in the 2θ range of 5-100º with step sizes of 0.0167º were used during data collection. In order to identify the reason of conductivity change,

thermal analyses of sample $LiCo_{0.5}Al_{0.5}O_2$ in air and 5%H_2/Ar were performed using a Stanton Redcroft STA/TGH series STA 1500 operating through a Rheometric Scientific system interface controlled by the software RSI Orchestrator in flowing air and 5% H_2/Ar at a flow rate of 50 ml/min. SEM observation was carried out on a HITACHI SU-6600 Field Emission Scanning Electron Microscope (FE-SEM).

The a.c. conductivity of $LiCo_{0.5}Al_{0.5}O_2$ in air was measured from 700 to 200 °C on cooling measured by a Solartron 1470E/1455 with applied frequency from 1MHz to 0.01Hz. The $LiCo_{0.5}Al_{0.5}O_2$ powders pre-fired at 800 °C was pressed into pellets with diameter of 13 mm and thickness around 2 mm then fired at 1050 °C for 1 hours. A silver coated pellet was fitted into the measuring apparatus and measurement was carried out in ambient air.

For oxygen concentration cell, air and pure oxygen were passing through 95% H_2SO_4 respectively before feeding into the two chambers of the cell. The voltage of the cell was recorded on a Solartron 1470E electrochemical interface. For hydrogen concentration cell, 5%H_2/Ar and pure hydroegn were passing through 95% H_2SO_4 respectively before feeding into the two chambers of the cell.

For fuel cell measurement, two types of cell was fabricated. Type A (sandwich type cell): the powder fired at 800 °C was mixed with 15 wt% starch. Three layer pellets with pure $LiCo_{0.5}Al_{0.5}O_2$ in the middle, $LiCo_{0.5}Al_{0.5}O_2$ mixed with 15wt% starch at the outer layers were pressed into 20mm in diameter. This is a sandwich structure with a dense layer in the middle with porous layers on each side. After firing at 1050 °C for 1 hour, the thickness of the middle layer was 100μm according to SEM observation (Figure S7A). The active area of the cell was 0.6 cm2 with overall thickness of 0.67mm. As for the electrode, it was found that platinum electrode may react with $LiCo_{0.5}Al_{0.5}O_2$ therefore silver paste was used as electrode for conductivity, concentration cell and fuel cell measurements. Diluted silver paste was used as cathode, anode and current collector. Type B cell (pellet type cell): a 1050 °C fired pellet with thickness of 0.79 mm was directly used as the electrolyte. Diluted silver paste mixed with a small amount of $LiCo_{0.5}Al_{0.5}O_2$ was used as both electrodes. The addition of $LiCo_{0.5}Al_{0.5}O_2$ is to introduce ionic conduction and reduce the electrode polarisation resistance. The active area of the cell with pellet electrolyte was 0.58 cm^2.

The cells were mounted on an alumina tube using a ceramic sealant for sealing. Hydrogen passing room temperature water was fed inside the tube and the cathode was exposed to open air. The flow rate of hydrogen was 50 ml/min. The a.c. impedance and I-V curve of the cell were recorded by a Solartron 1470E/1455 electrochemical interface.

Supporting Information

Supporting Information is available from the Wiley Online Library or from the author.

Acknowledgements

The authors thank EPSRC SuperGen Fuel Cells (EP/G030995/1), Flame SOFCs (EP/K021036/1) and UK-India Biogas SOFCs (EP/I037016/1) projects for funding.

References

[1] T. Norby, *Solid State Ionics* **1999**, *125*, 1.
[2] D. A. Boysen, S. M. Haile, H. J. Liu, R. A. Secco, *Chem. Mater.* **2003**, *15*, 727.
[3] T. Kenjo, Y. Ogawa, *Solid State Ionics* **1995**, *76*, 29.
[4] H. B. Wang, C. Tealdi, U. Stimming, K. L. Huang, L. Q. Chen, *Electrochim. Acta* **2009**, *54*, 5257.
[5] X. L. Chen, X. Li, S. A. Jiang, C. R. Xia, U. Stimming, *Electrochim. Acta* **2006**, *51*, 6542.
[6] Y. Z. Jiang, X. X. Xu, R. Lan, L. Zhang, S. W. Tao, *J. Alloy. Compd.* **2009**, *480*, 874.
[7] M. Nagao, T. Kamiya, P. Heo, A. Tomita, T. Hibino, M. Sano, *J. Electrochem. Soc.* **2006**, *153*, A1604.
[8] X. Wu, A. Verma, K. Scott, *Fuel Cells* **2008**, *8*, 453.
[9] X. L. Chen, C. S. Wang, E. A. Payzant, C. R. Xia, D. Chu, *J. Electrochem. Soc.* **2008**, *155*, B1264.
[10] S. W. Tao, *Solid State Ionics* **2009**, *180*, 148.
[11] X. X. Xu, S. W. Tao, P. Wormald, J. T. S. Irvine, *J. Mater. Chem.* **2010**, *20*, 7827.
[12] D. A. Boysen, S. M. Haile, H. J. Liu, R. A. Secco, *Chem. Mater.* **2003**, *15*, 727.
[13] H. Iwahara, T. Esaka, H. Uchida, N. Maeda, *Solid State Ionics* **1981**, *3-4*, 359.
[14] K. D. Kreuer, *Annual Rev. Mater. Res.* **2003**, *33*, 333.
[15] L. Malavasi, C. A. J. Fisher, M. S. Islam, *Chem. Soc. Rev.* **2010**, *39*, 4370.
[16] E. Fabbri, D. Pergolesi, E. Traversa, *Chem Soc Rev* **2010**, *39*, 4355.
[17] S. W. Tao, J. T. S. Irvine, *Adv. Mater.* **2006**, *18*, 1581.
[18] L. Yang, S. Z. Wang, K. Blinn, M. F. Liu, Z. Liu, Z. Cheng, M. L. Liu, *Science* **2009**, *326*, 126.
[19] Y. Yamazaki, R. Hernandez-Sanchez, S. M. Haile, *Chem. Mater.* **2009**, *21*, 2755.
[20] C. Zuo, S. Zha, M. Liu, M. Hatano, M. Uchiyama, *Adv. Mater.* **2006**, *18*, 3318.
[21] R. Haugsrud, T. Norby, *Nat. Mater.* **2006**, *5*, 193.
[22] R. Haugsrud, T. Norby, *Solid State Ionics* **2006**, *177*, 1129.
[23] D. J. D. Corcoran, D. P. Tunstall, J. T. S. Irvine, *Solid State Ionics* **2000**, *136*, 297.
[24] C. E. Tambelli, J. P. Donoso, C. J. Magon, A. C. D. Ângelo, A. O. Florentino, M. J. Saeki, *Solid State Ionics* **2000**, *136-137*, 243.
[25] J. B. Goodenough, A. Manthiram, B. Wnetrzewski, *J. Power Sources* **1993**, *43*, 269.
[26] A. R. Armstrong, P. G. Bruce, *Nature* **1996**, *381*, 499.
[27] A. S. Arico, P. Bruce, B. Scrosati, J. M. Tarascon, W. Van Schalkwijk, *Nat. Mater.* **2005**, *4*, 366.
[28] J. Fan, P. S. Fedkiw, *J. Power Sources* **1998**, *72*, 165.
[29] M. Butel, L. Gautier, C. Delmas, *Solid State Ionics* **1999**, *122*, 271.
[30] S. W. Tao, J. T. S. Irvine, *Nat. Mater.* **2003**, *2*, 320.
[31] K. Terakura, A. R. Williams, T. Oguchi, J. Kubler, *Phys. Rev. Lett.* **1984**, *52*, 1830.
[32] M. N. Khan, J. Bashir, *Mater. Res. Bull.* **2006**, *41*, 1589.
[33] L. Giorgi, M. Carewska, S. Scaccia, E. Simonetti, E. Giacometti, R. Tulli, *Inter. J. Hydrogen Energy* **1996**, *21*, 491.
[34] S. W. Tao, Q. Y. Wu, Z. L. Zhan, G. Y. Meng, *Solid State Ionics* **1999**, *124*, 53.
[35] Z. Y. Wen, Z. H. Gu, X. H. Xu, X. J. Zhu, *J. Nuclear Mater.* **2004**, *329*, 1283.
[36] A. V. Kolobov, A. Rogalev, F. Wilhelm, N. Jaouen, T. Shima, J. Tominaga, *Appl. Phys. Lett.* **2004**, *84*, 1641.
[37] D. Pergolesi, E. Fabbri, A. D'Epifanio, E. Di Bartolomeo, A. Tebano, S. Sanna, S. Licoccia, G. Balestrino, E. Traversa, *Nat. Mater.* **2010**, *9*, 846.
[38] B. C. H. Steele, A. Heinzel, *Nature* **2001**, *414*, 345.

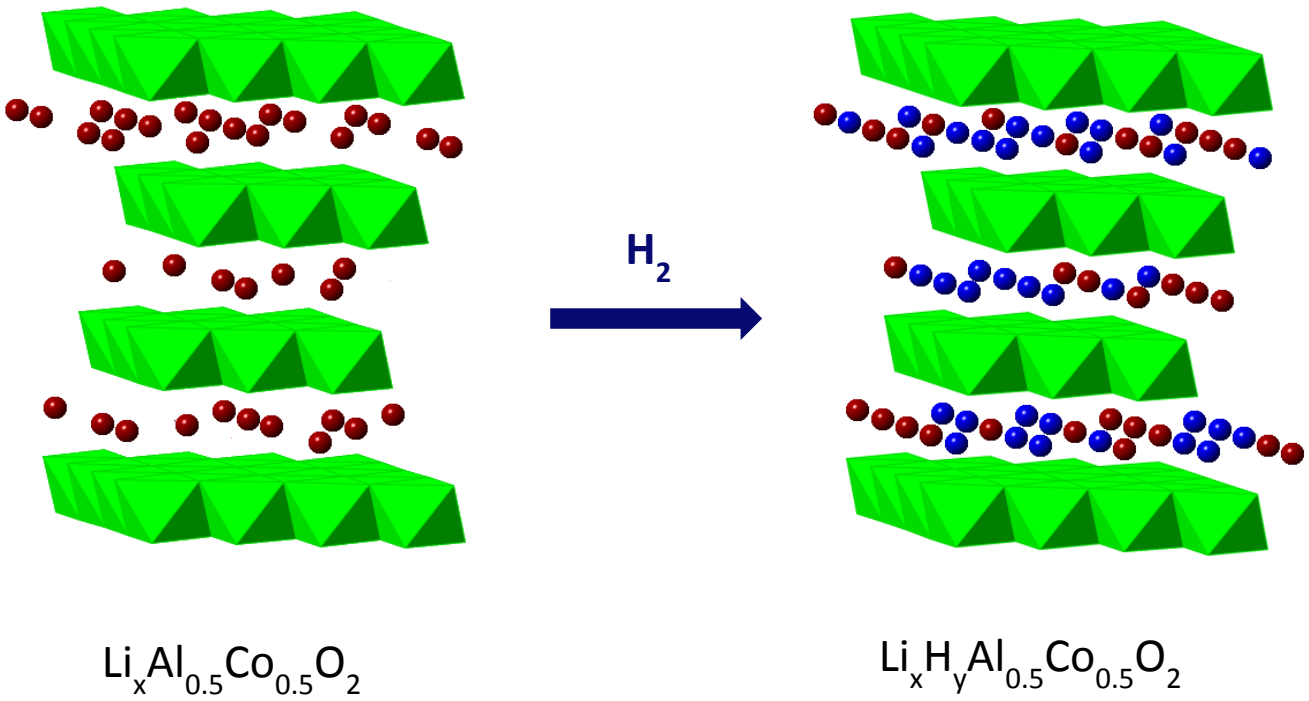

Figure 1 Diagram for insertion of protons in the $Li_xAl_{0.5}Co_{0.5}O_2$ in the presence of hydrogen. Red sphere, Li^+ ions; blue sphere, H^+ ions.

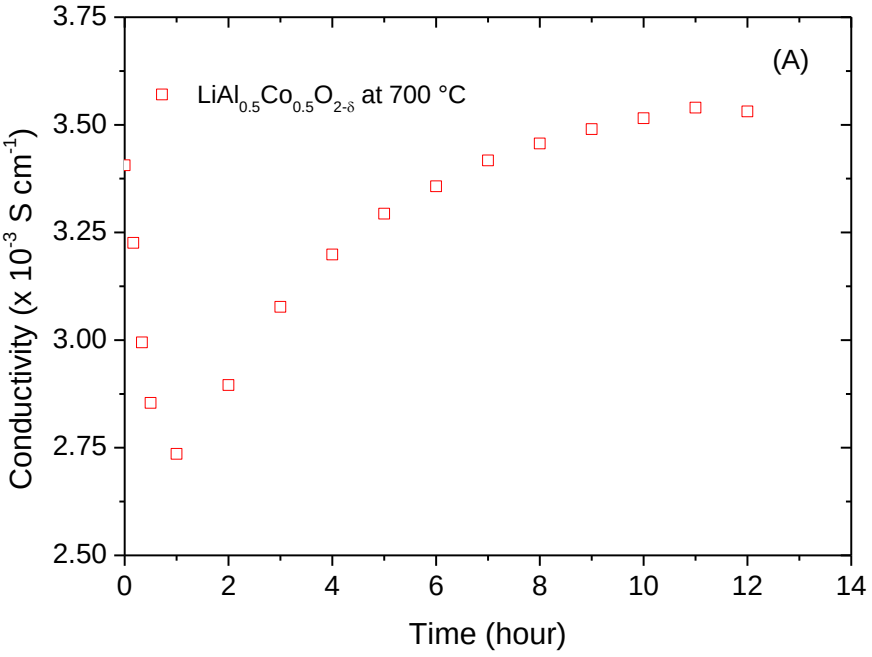

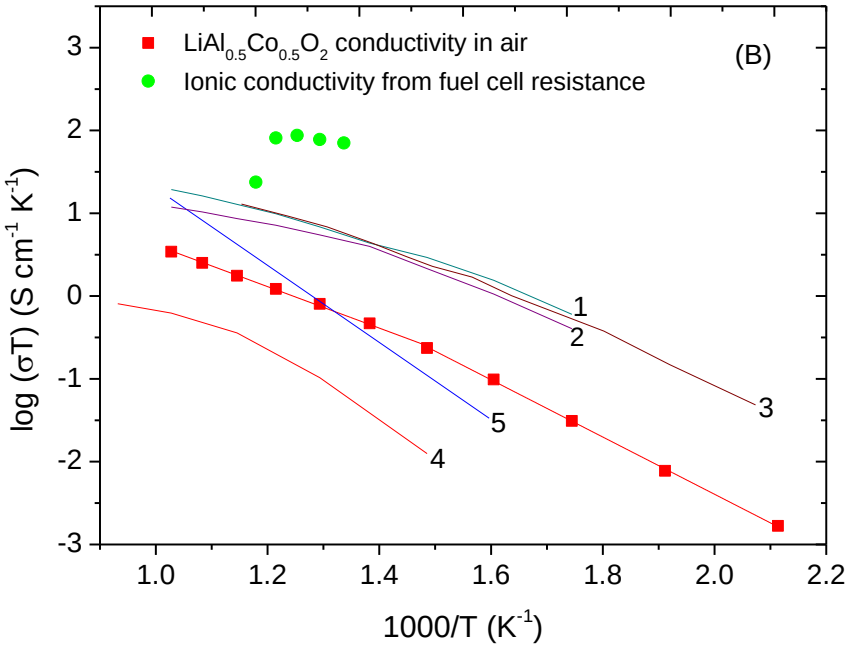

Figure 2 The conductivity of nominal $LiAl_{0.5}Co_{0.5}O_2$ in air at 700 °C (A) and at different temperature (Legend information for Figure 2B: 1 $BaCe_{0.7}Zr_{0.1}Y_{0.2}O_{3-\delta}$ (ref. 20); 2 $BaCe_{0.5}Zr_{0.3}Y_{0.16}Zn_{0.04}O_{3-\delta}$ (ref. 17); 3. $BaZr_{0.8}Y_{0.2}O_{3-\delta}$ (ref. 19); 4 $La_{0.99}Ca_{0.01}NbO_4$ (ref. 21); 5 $(ZrO_2)_{0.9}(Y_2O_3)_{0.1}$ (ref. 38).

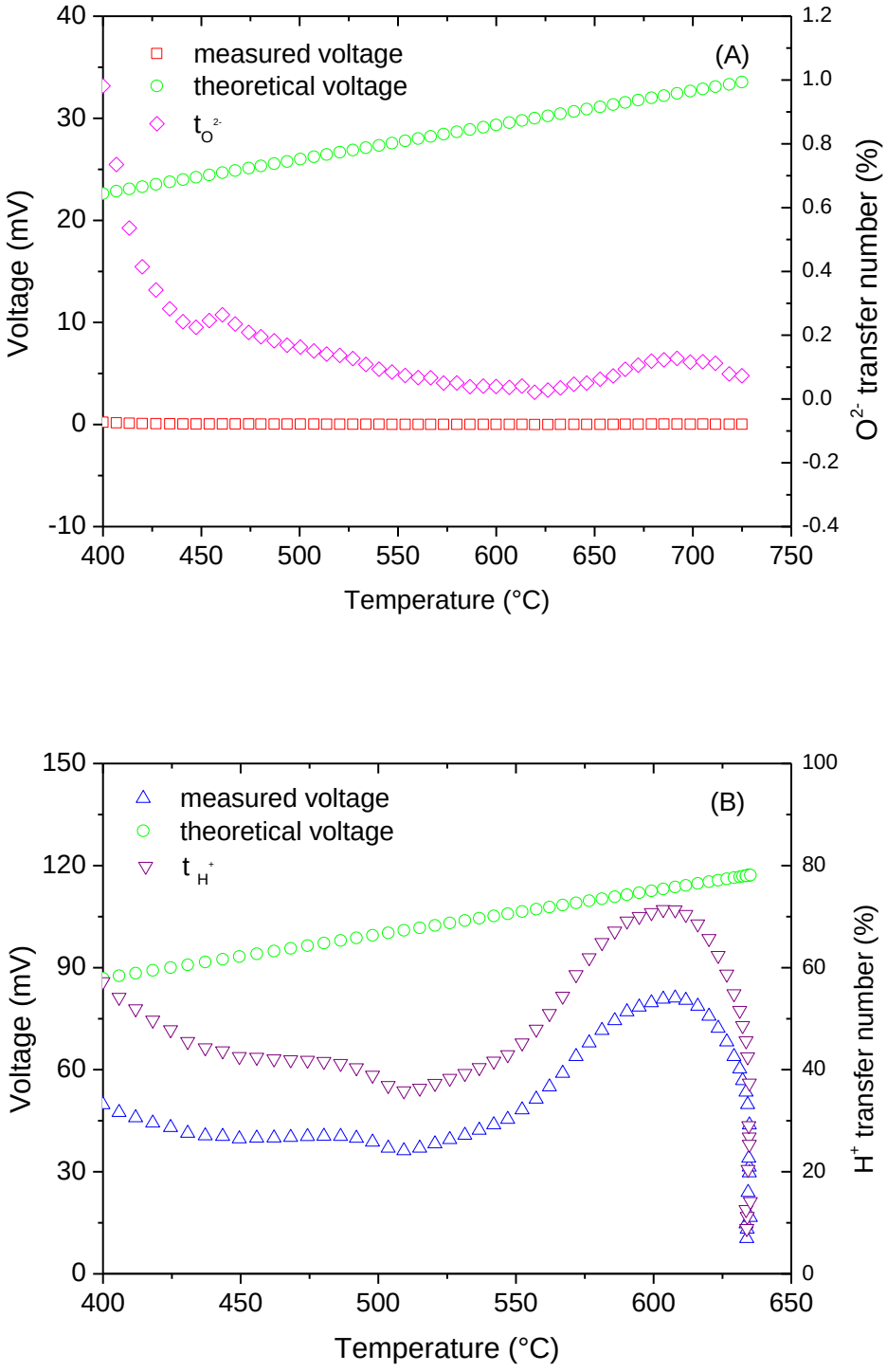

Figure 3 The observed OCV, theoretical OCV and transfer number from oxygen concentration cell (A) and hydrogen concentration cell (B).

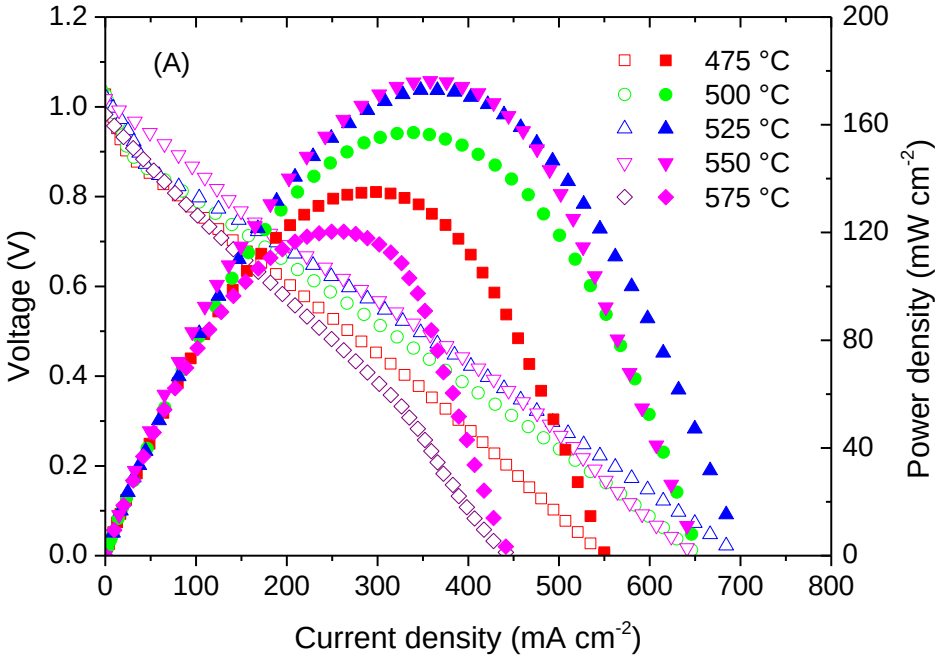

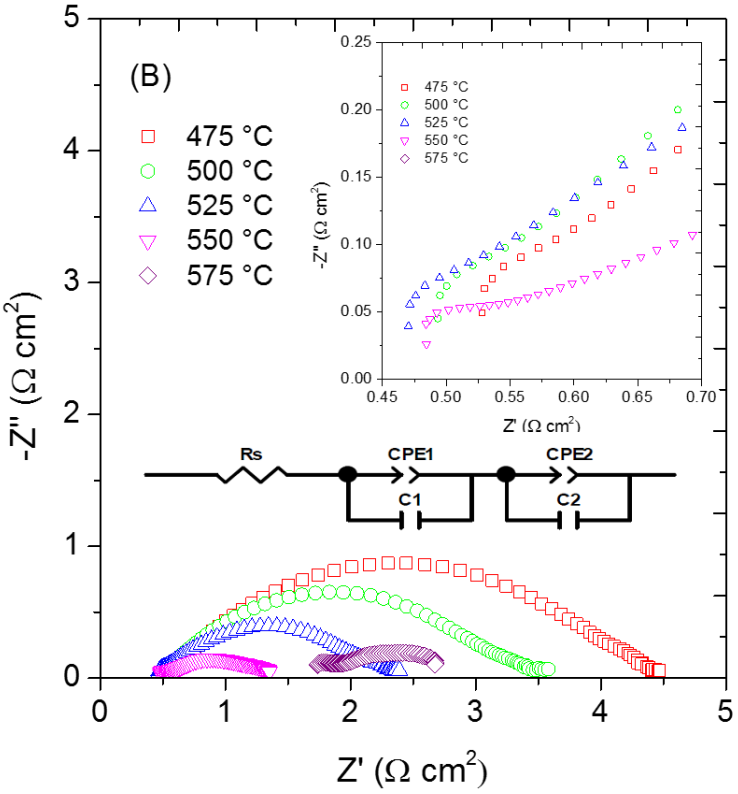

Figure 4 The fuel cell performance (A) and a.c. impedance spectra at OCV of the cell (B) at different temperatures using $LiAl_{0.5}Co_{0.5}O_2$ thick pellet as the electrolyte.

Supporting Online Materials

Table S1 Structure parameters of nominal $LiAl_{0.5}Co_{0.5}O_2$.

Atom	Site	Occupancy	*x*	*y*	*z*	$U_{iso}/Å^2$
Li	3a	1	0	0	0	0.012(11)
Al	3b	0.5	0	0	0.5	0.0046(24)
Co	3b	0.5	0	0	0.5	0.0046(24)
O	6c	1	0	0	0.2400(4)	0.004(7)

Note: Space group $R\bar{3}m(166)$; a = 2.8016(7) Å, c = 14.1631 (34) Å, V = 96.28(4) Å^3. R_{wp} = 2.96%, R_p = 2.29%, χ_{red}^2 = 1.287.

Table S2 Structure parameters of nominal $Li_{0.9}Al_{0.5}Co_{0.5}O_2$.

Atom	Site	Occupancy	*x*	*y*	*z*	$U_{iso}/Å^2$
Li	3a	1	0	0	0	0.011(14)
Al	3b	0.5	0	0	0.5	0.0128(23)
Co	3b	0.5	0	0	0.5	0.0128(23)
O	6c	1	0	0	0.2413(5)	0.004(4)

Note: Space group $R\bar{3}m(166)$; a = 2.8016(1) Å, c = 14.1608 (6) Å, V = 96.26(1) Å^3. R_{wp} = 3.21%, R_p = 2.42%, χ_{red}^2 = 1.463.

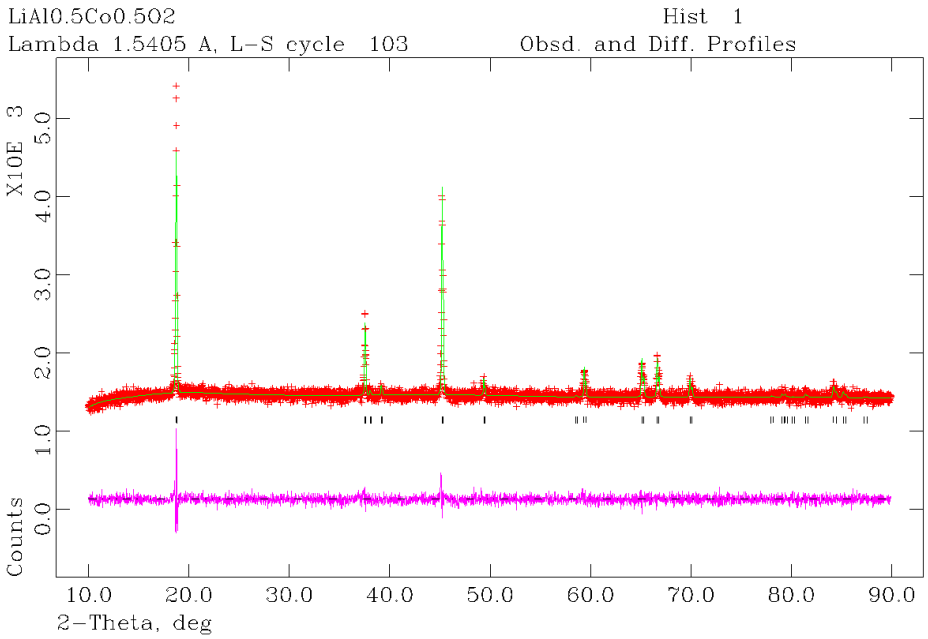

Figure S1 XRD pattern of nominal $LiAl_{0.5}Co_{0.5}O_2$.

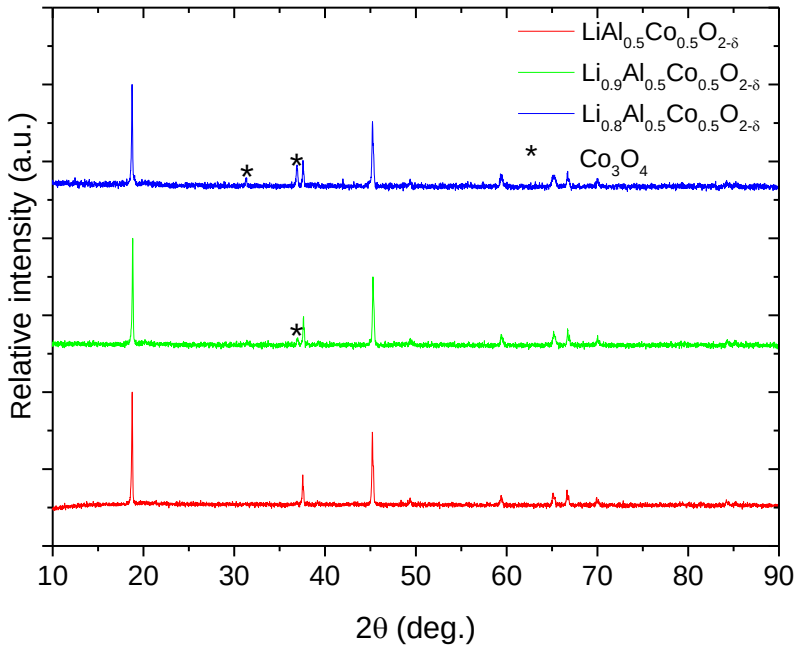

Figure S2 The XRD pattern of samples with nominal compositions $Li_xAl_{0.5}Co_{0.5}O_2$ at x = 0.8 – 1.0. * Co_3O_4: 01-080-1541.

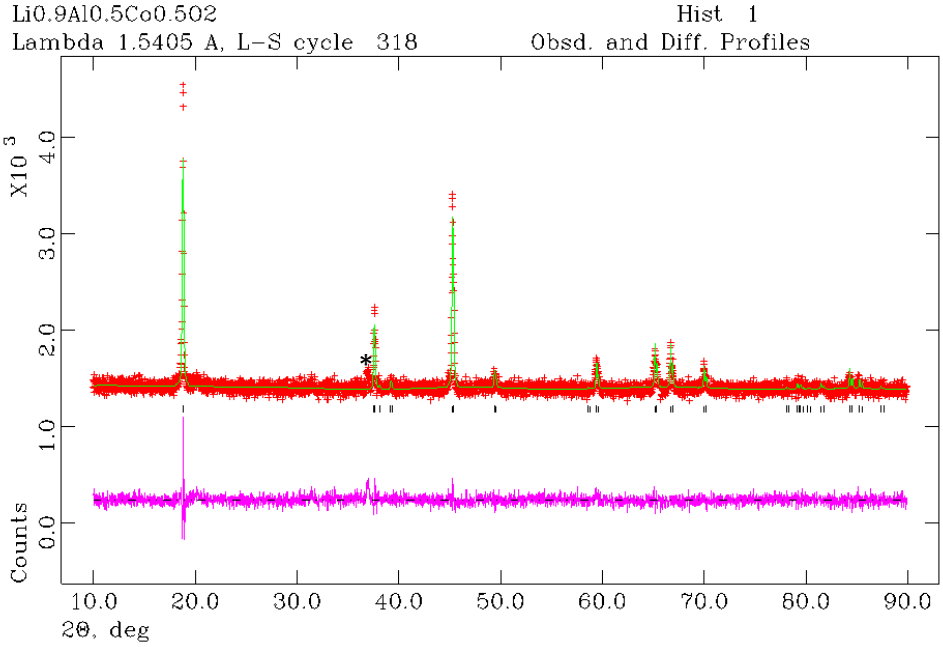

Figure S3 XRD pattern of nominal $Li0.9Al_{0.5}Co_{0.5}O_2$. * Co_3O_4

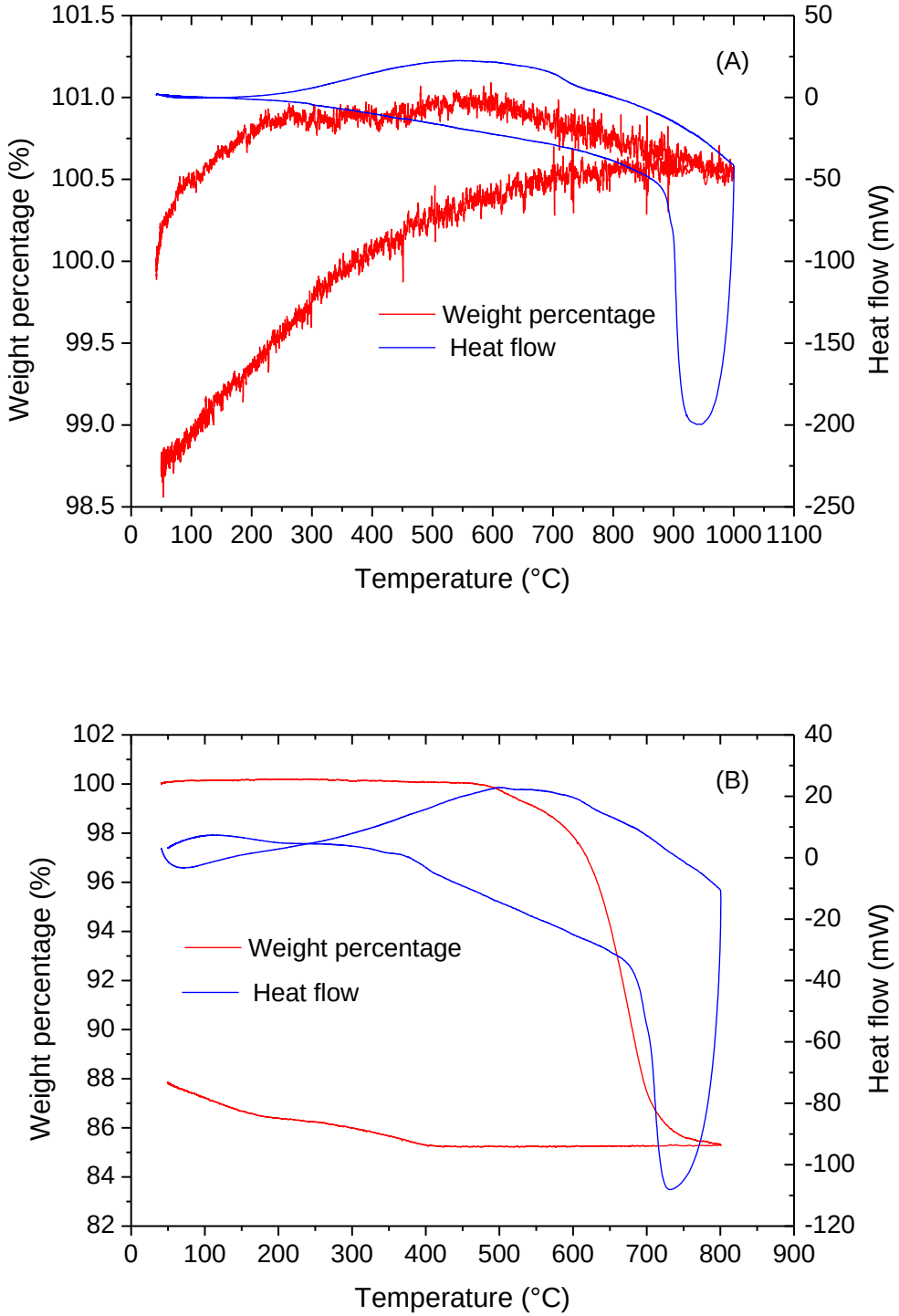

Figure S4 Thermal analyses of the nominal $LiAl_{0.5}Co_{0.5}O_2$ in air (A) and 5%H_2/Ar (B).

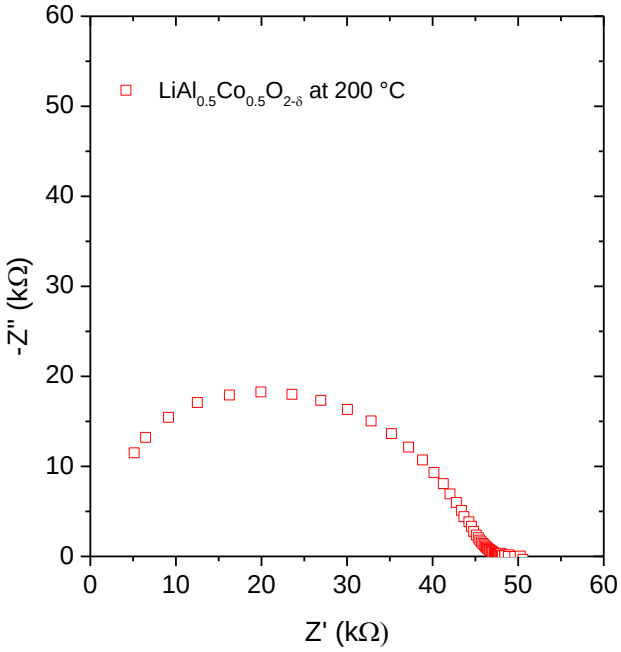

Figure S5 The a.c. impedance spectrum of LiAl0.5Co0.5O2 in air at 200 °C .

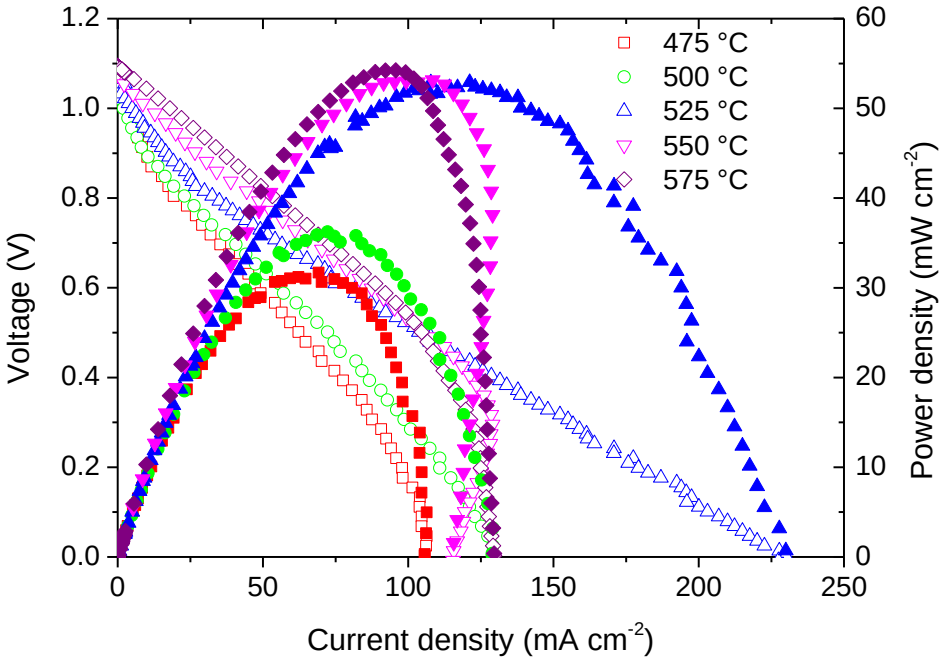

Figure S6 The fuel cell performance at different temperatures using $LiAl_{0.5}Co_{0.5}O_2$ as the electrolyte with sandwich structure.

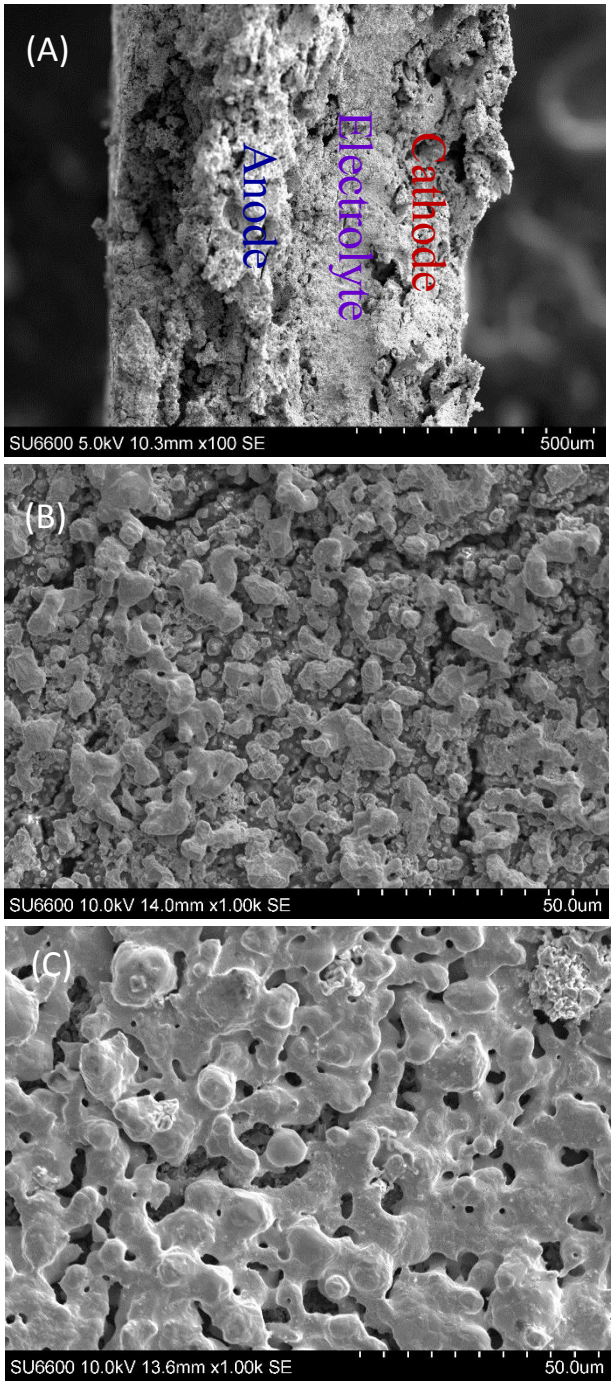

Figure S7 SEM pictures of the sandwich type cell after H_2/air fuel cell measurements, the cross section (A), anode surface (B) and cathode surface (C).

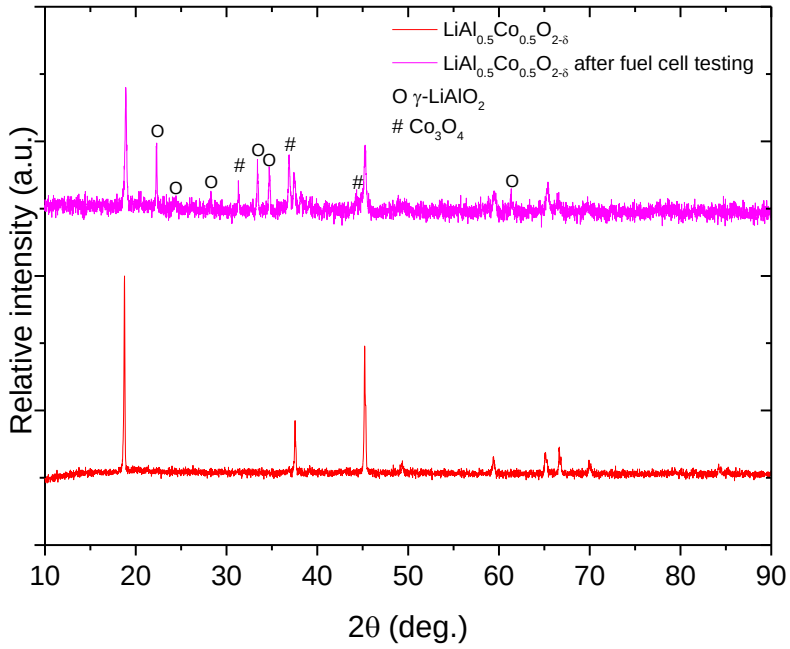

Figure S8 The XRD pattern of $LiAl_{0.5}Co_{0.5}O_2$ before and after H_2/air fuel cell measurements. After fuel cell testing, it contains impurities γ-$LiAlO_2$ (JCPDS 01-073-1338) and Co_3O_4 (JCPDS 01-076-1802).